

Chapter 4: Results for the DCS

4.1 Introduction

The required development research was outlined in Chapter 3 and a DCS solution was presented. The following chapter covers the verification of the DCS solution with theoretical and actual data. It also shows what the DCS user interface looks like.

4.2 Network solver

Two network-solving packages are used to test the DCS's network solver, namely Flownex 7.012-Demo Version⁸ and KYPipe⁹.

4.2.1 Theoretical network solver verification

For illustration purposes, all the pipes in this section are 1 000 m long, 0.6 m in diameter and have a roughness of 45 μm . The output results are shown in Appendix C.

The first setup that will be solved is simple. It is obvious that \dot{m}_1 and \dot{m}_2 has to be equal.

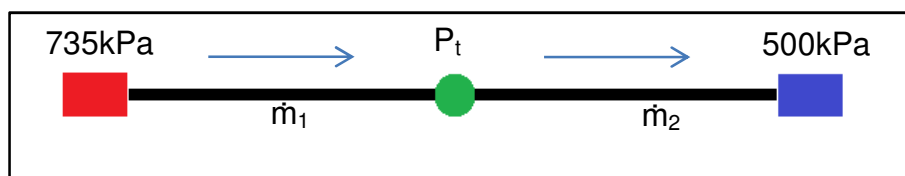


Figure 32: Two pipes with one intermediate node

⁸ Flownex, <http://www.flownex.com/>.

⁹ KYpipe, <http://kypipe.com/>.

	KPipe	Flownex	DCS	KYPipe % comparison	Flownex % comparison
P_t (kPa)	629.9	629.33	628.48	99.77	99.86
\dot{m}_1 (kg/s)	115.1	118.59	118.58	97.07	99.99
\dot{m}_2 (kg/s)	115.1	118.59	118.58	97.07	99.99

Table 5: Simulation results for two pipes with one intermediate node

From the results in Table 5, the DCS network solver differs with a maximum of 2.93% and 0.14% from KYPipe and Flownex respectively.

The following setup in Figure 33 is the same as the one discussed in section 3.6.3, except that the fluid and pipe properties for this situation are all calculated and not kept constant.

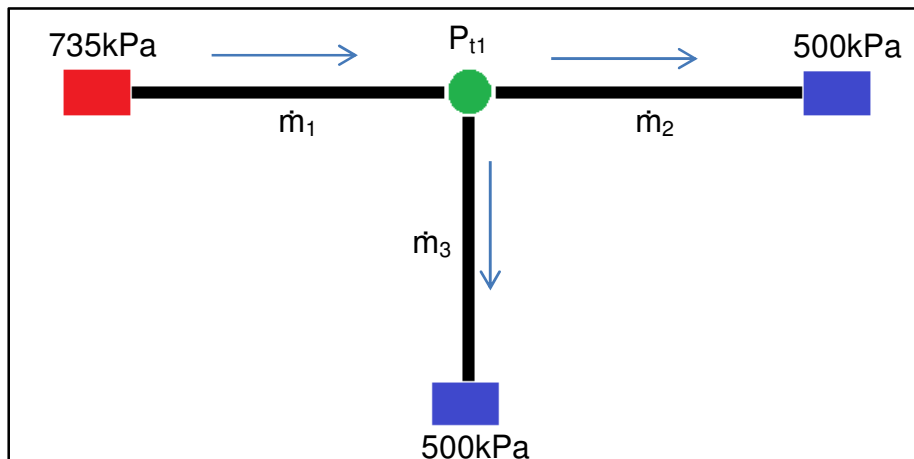


Figure 33: Three pipes with one intermediate node

	KPipe	Flownex	DCS	KYPipe % comparison	Flownex % comparison
P_{t1} (kg/s)	554.6	555.06	555.8	99.78	99.87
m_1 (kg/s)	103.8	106.46	105.76	98.15	99.34
m_2 (kg/s)	51.9	53.23	52.93	98.05	99.44
m_3 (kg/s)	51.9	53.23	52.93	98.05	99.44

Table 6: Simulation results for three pipes with one intermediate node

From the results in Table 6 the DCS network solver differs with a maximum of 1.95% and 0.66% from KYPipe and Flownex respectively. For the majority of mining compressed air networks, the setup in Figure 33 will form the main building block of the solver. It seldom happens that more than three pipes are connected at a single node. The setup shown in Figure 34 is essentially two of the setups shown in Figure 33 combined.

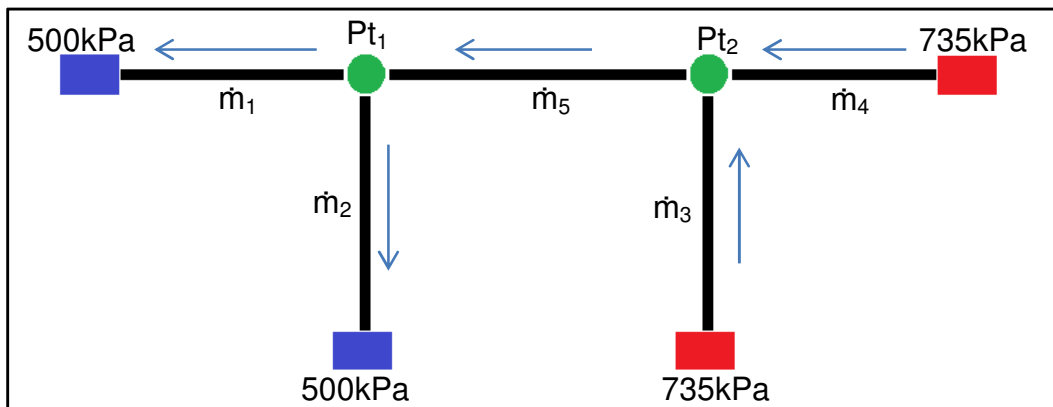


Figure 34: Five pipes with two intermediate nodes

	KPipe	Flownex	DCS	KYPipe % comparison	Flownex % comparison
P_{t1} (kPa)	546.2	546.36	546.82	99.89	99.92
P_{t2} (kPa)	701.6	701.35	700.86	99.89	99.93
m_1 (kg/s)	47.4	48.6	48.21	98.32	99.20
m_2 (kg/s)	47.6	48.6	48.21	98.73	99.20
m_3 (kg/s)	95	97.2	96.32	98.63	99.09
m_4 (kg/s)	47.5	48.6	48.21	98.53	99.20
m_5 (kg/s)	47.5	48.6	48.21	98.53	99.20

Table 7: Simulation results for five pipes with two intermediate nodes

This setup is more complex than the previous two and still compares well with the other two solving packages.

To test the DCS network solver, it is given a setup to solve that is not likely to be encountered on a mine's compressed air network. Figure 35 shows 21 pipes with nine intermediate nodes.

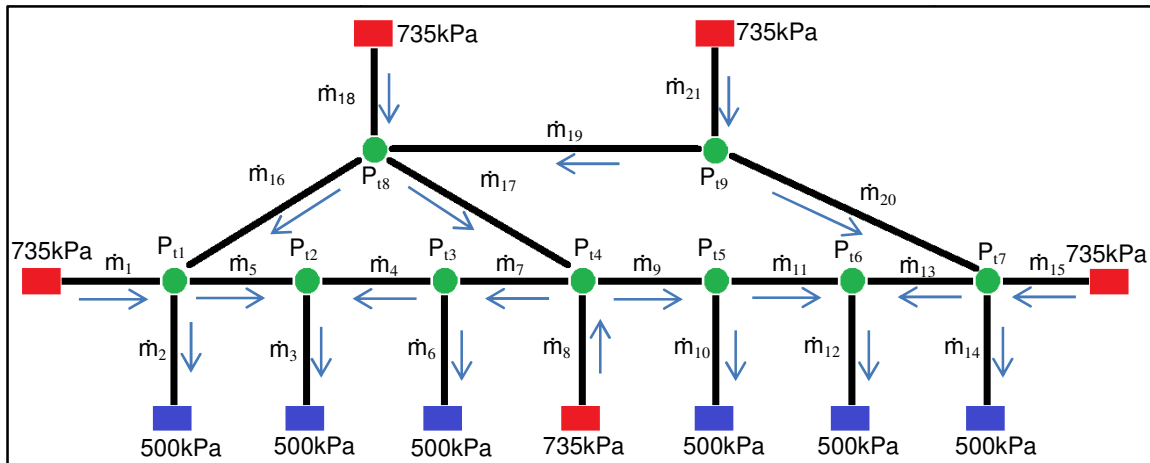


Figure 35: Twenty-one pipes with nine intermediate nodes

The demo version of Flownex does not allow more than ten pipes and ten nodes to be used in a simulation. For this reason, the following scenario will only be compared with KYPipe.

	KPipe	DCS	KYPipe % comparison		KPipe	DCS	KYPipe % comparison		KPipe	DCS	KYPipe % comparison
P_{t1} (kPa)	620.9	619.9	99.84	\dot{m}_1 (kg/s)	85.2	86.7	98.27	\dot{m}_{11} (kg/s)	2.6	2.6	100.00
P_{t2} (kPa)	566.4	566.3	99.98	\dot{m}_2 (kg/s)	79.1	80.3	98.51	\dot{m}_{12} (kg/s)	58	58.3	99.49
P_{t3} (kPa)	566.8	566.5	99.95	\dot{m}_3 (kg/s)	57.6	58	99.31	\dot{m}_{13} (kg/s)	55.4	55.8	99.28
P_{t4} (kPa)	632.4	632.3	99.98	\dot{m}_4 (kg/s)	3	3.12	96.15	\dot{m}_{14} (kg/s)	37.2	38.1	97.64
P_{t5} (kPa)	567	567	100.00	\dot{m}_5 (kg/s)	54.5	55	99.09	\dot{m}_{15} (kg/s)	79.7	81.1	98.27
P_{t6} (kPa)	567.4	566.9	99.91	\dot{m}_6 (kg/s)	57.7	58.2	99.14	\dot{m}_{16} (kg/s)	48.4	48.8	99.18
P_{t7} (kPa)	621.8	621.9	99.98	\dot{m}_7 (kg/s)	60.8	61.4	99.02	\dot{m}_{17} (kg/s)	40	40.4	99.01
P_{t8} (kPa)	659.3	659.1	99.97	\dot{m}_8 (kg/s)	81.2	82.2	98.78	\dot{m}_{18} (kg/s)	70.6	71.2	99.16
P_{t9} (kPa)	664.7	664.4	99.95	\dot{m}_9 (kg/s)	60.4	61.1	98.85	\dot{m}_{19} (kg/s)	17.8	17.9	99.44
				\dot{m}_{10} (kg/s)	57.8	58.4	98.97	\dot{m}_{20} (kg/s)	50.3	51	98.63
								\dot{m}_{21} (kg/s)	68.2	68.8	99.13

Table 8: Simulation results for 21 pipes with nine intermediate nodes

From the scenario in Figure 35, it is clear that for a complex system, the DCS solver gives accurate results.

4.2.2 Comparing the DCS network solver to actual network data

The minor pipe losses were determined using average historical flow and pressure data for one month. Historical data for compressor house pressures and shaft flows were used as input values.

The minor loss coefficient for each pipe was manually varied until the output shaft pressures corresponded with the historically logged shaft pressures. Figure 36 (not drawn to scale) shows the minor loss coefficients for the network. The three shafts at the bottom of Figure 5 were combined to form one node. Only the middle shaft of the three has a pressure transmitter and the sum of the three shaft flows were used. The blue and red rectangles represent shafts and compressor houses respectively.

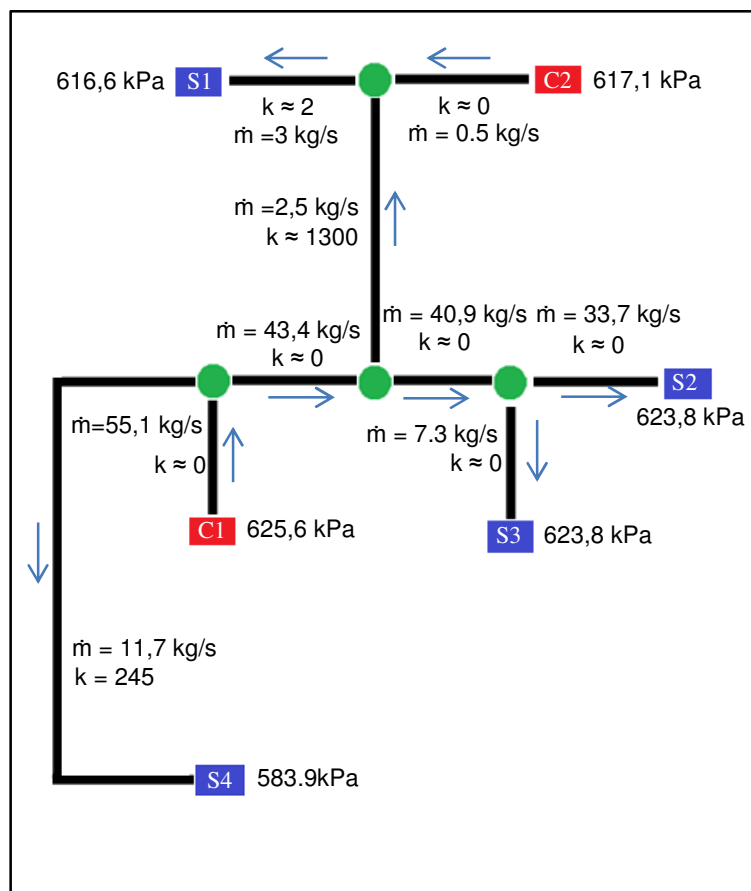


Figure 36: Estimated minor pipe losses

The geometry loss factors are close to zero where pipe lengths are relatively small or where the pipes do not have significant misalignment. Pipe friction losses are still present.

To verify the minor loss coefficients, a set of logged historical compressor house pressure and shaft flows were given to the DCS as input values. Figure 37 shows the shaft pressures that were obtained.

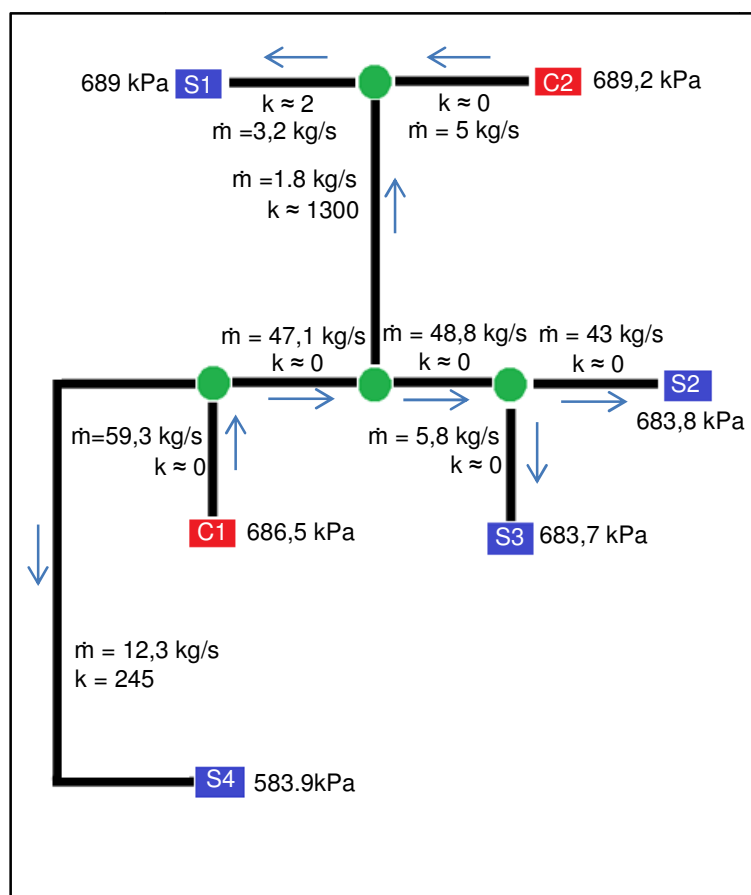


Figure 37: DCS shaft pressures obtained by using estimated minor pipe losses

Table 9 shows the accuracy of the pressures calculated by the DCS.

	S1	S2	S3	S4
Measured shaft pressure (kPa)	688.20	680.10	680.10	635.90
DCS calculated pressure (kPa)	689.00	683.80	683.70	641.70
Accuracy (%)	99.88	99.46	99.47	99.09

Table 9: Actual and DCS shaft pressures

4.3 Compressor selection

Figure 38 shows the logged historical power consumption and mass flow of the compressors for a production day at the mine.

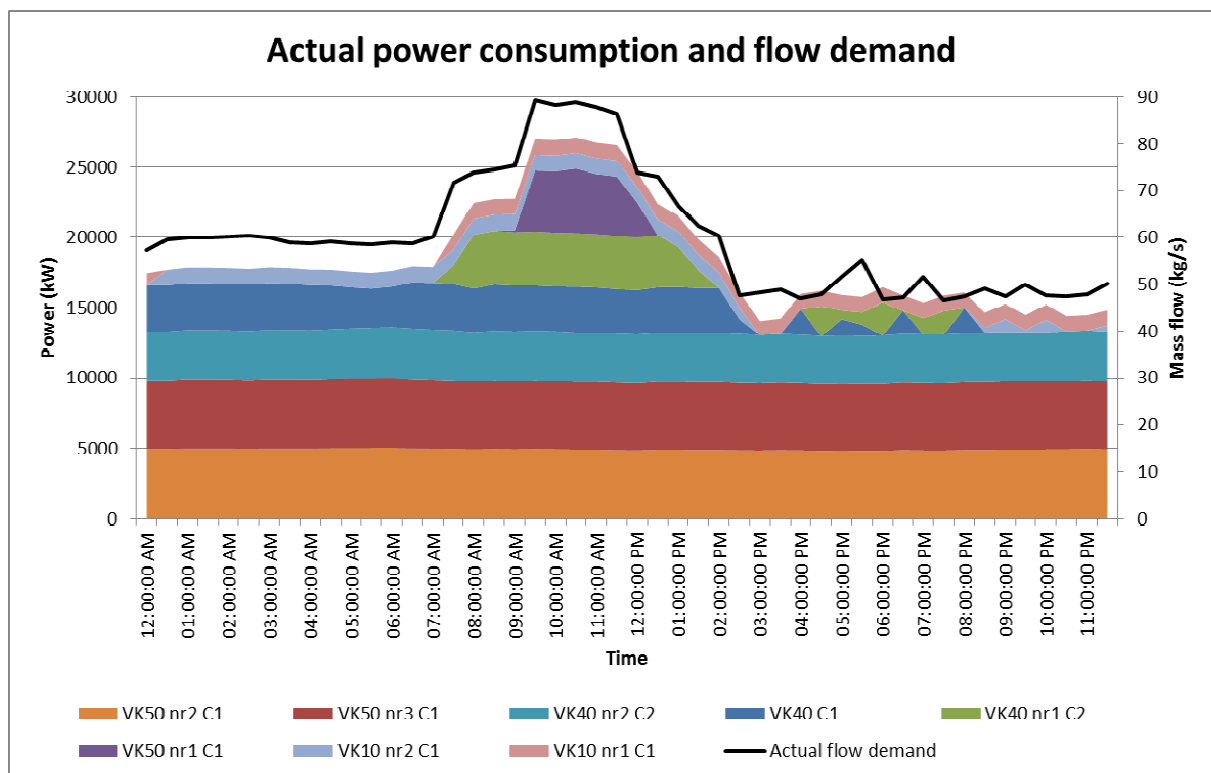


Figure 38: Power consumption and demand flow

From Figure 38 it is clear that there is compressor cycling for this day, especially in the afternoon and evening.

Using the selection method discussed in section 3.7, the following theoretical power consumption graph was obtained:

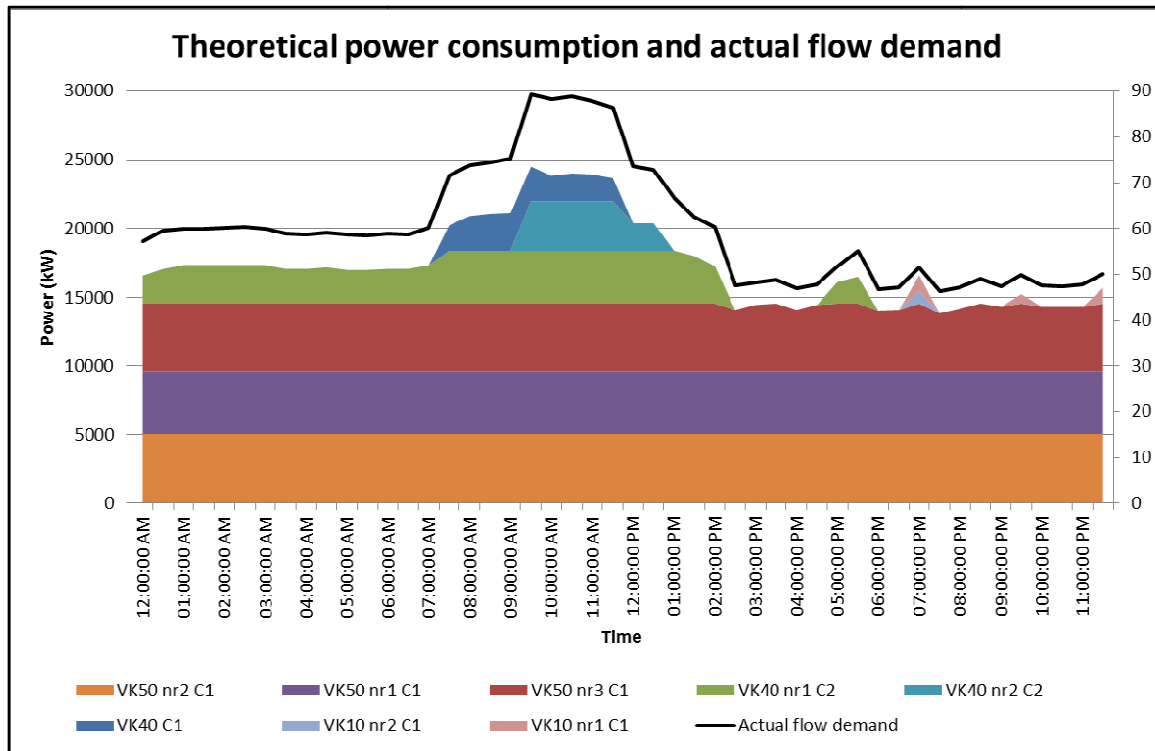


Figure 39: Theoretical power consumption and actual demand flow

The figure shows that with the DCS selection method, compressor cycling is not eliminated. However, the actual number of starts and stops for all the compressors for this day was reduced from 24 to 14 by the DCS (Appendix D).

The theoretical DCS day average power required to supply the compressed air demand is 1 072 kW less than the present master controller required.

4.4 Pressure set point control

Due to labour unrest, the implementation of the DCS on the case study was delayed. The surface control valves were therefore not installed before the completion of this dissertation. An assumption is made that a shaft has a resistance to flow. During the drilling shift, the shaft resistance is smaller than at other times of the day when less

equipment is used. This resistance varies constantly, but can be used to determine how a shaft's flow would have reacted for the exact same conditions. Equation 4.1 shows Bernoulli's Equation rewritten.

$$\Delta P = S_{\text{resistance}} \frac{\rho_{\text{ave}} v^2}{2} \quad 4.1$$

with the shaft surface pressure and fluid velocity known from logged historical data and the exit pressure being the average underground mine atmospheric pressure.

The average atmospheric pressure of the shaft is assumed to be 95 kPa. The density is obtained by using the average of the shaft's surface pressure and atmospheric pressure. After the shaft resistance is calculated, the effect of lowering the shaft surface pressure can be determined by rewriting Equation 4.2.

$$v = \sqrt{\frac{2\Delta P}{\rho_{\text{atm}} * S_{\text{resistance}}}} \quad 4.2$$

By using the same day as in section 4.3, the results are shown in Figure 40 on the following page.

No pressure control is done during the drilling shift between 05:00 and 14:00 so that there is no interference with production. From 02:00 to 05:00 and 14:00 to 18:00, the pressure was reduced to 400 kPa to ensure a positive pressure for the refuge bays. From 18:00 to 02:00, the pressure was lowered to 500 kPa so that certain pneumatic equipment used for ore extraction could function properly.

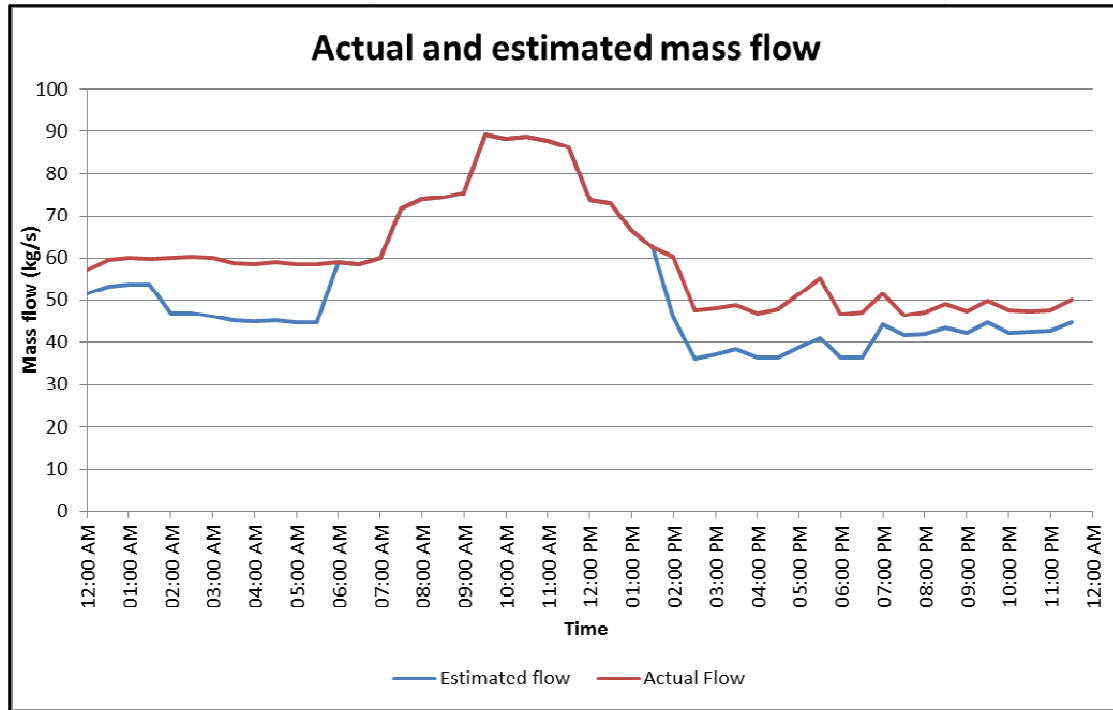


Figure 40: Actual and estimated mass flow for the network

The new calculated shaft flows¹⁰ are then used by the network solver to determine the minimum pressure set point required at the compressor house(s). For instance at 02:30, when all the shaft surface control valves are set to reduce pressures to 400 kPa, the DCS network-solver determined that the compressor set point can be reduced to 430 kPa. This is the minimum pressure required to supply adequate compressed air to Shaft 4 (S4), as shown in Figure 41 on the following page.

The pressures shown are the theoretical pressures just before the surface control valves. In this instance, S4 is the shaft that determines the minimum compressor house pressure set point for the specified conditions. The compressor house

¹⁰ For the actual implementation of DCS, these flows would be the measured shaft flows after the surface control valves have reduced each shaft's pressure

pressure set point will always be high enough to ensure that shaft pressure schedules are satisfied.

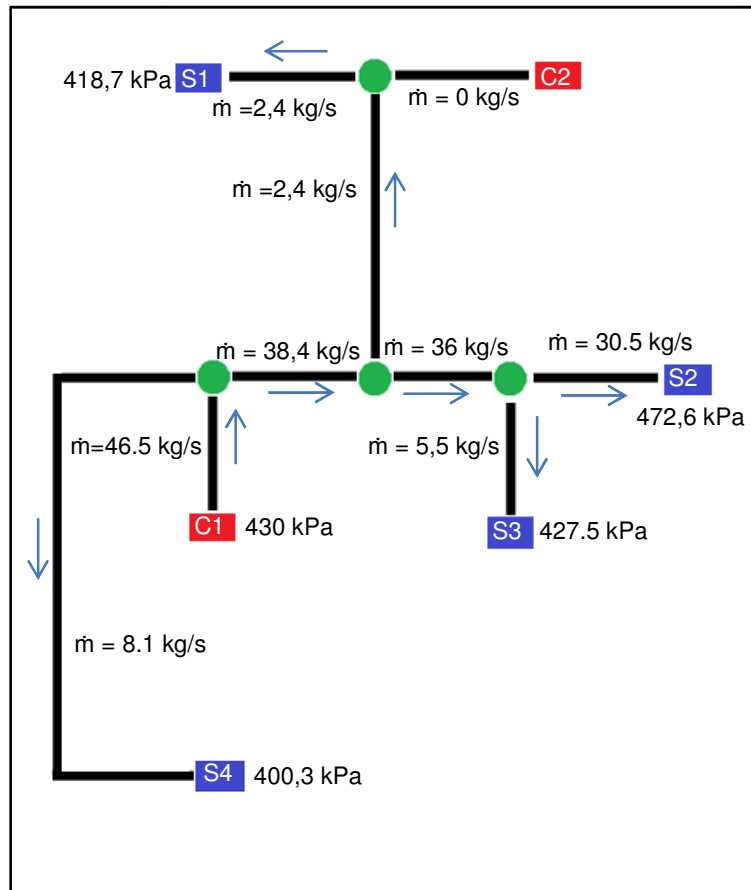


Figure 41: Required compressor pressure set point

Figure 42 shows the resulting power consumption caused by the reduced flow.

This reduction in pressure during certain times of the day resulted in a power saving of 2 596 kW (Appendix D).

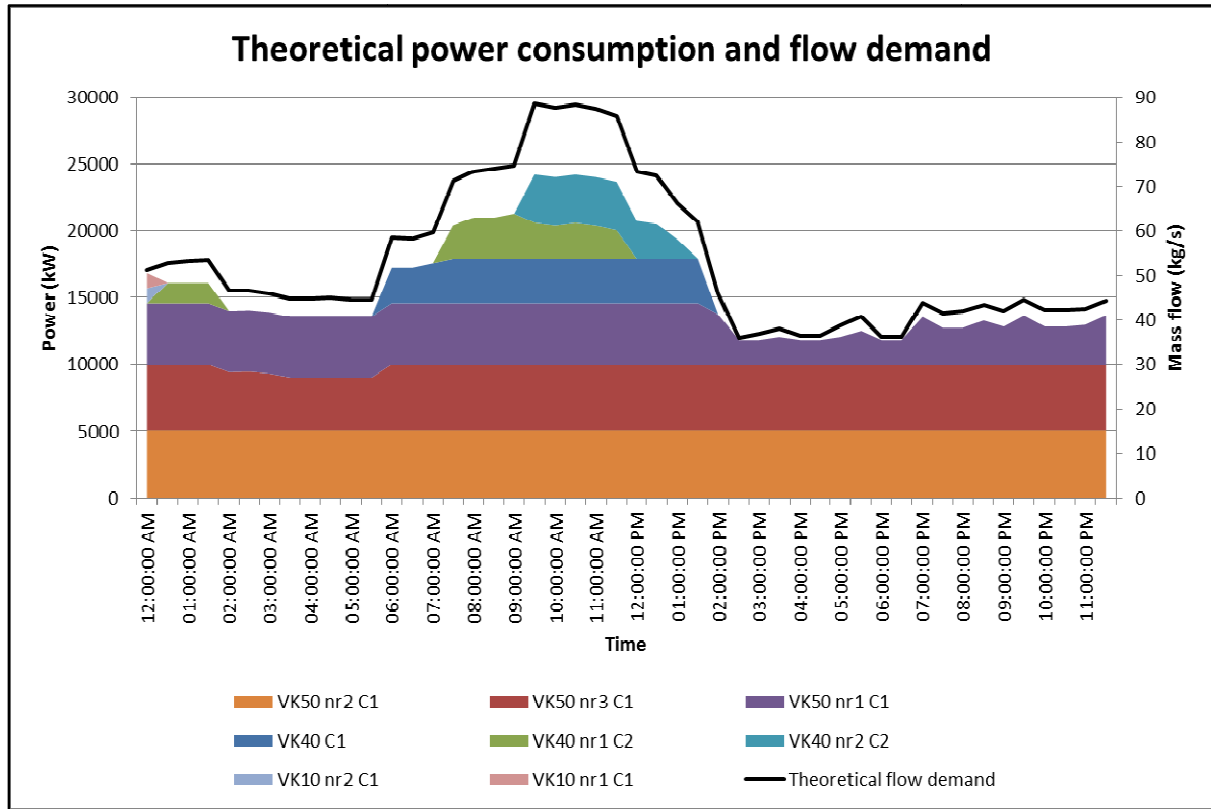


Figure 42: Theoretical power consumption and flow demand

4.5 DCS interface

Visual Basic .NET¹¹ was used for the initial network solving development [38]. The Visual Basic .NET code for the DCS network solver is shown in Appendix B. After the abilities of the DCS were proven, the Visual Basic .NET code was translated to Delphi¹² and incorporated into the user-friendly REMS platform by a software development team.

¹¹ Visual Basic .NET developed by Microsoft, <http://msdn.microsoft.com/en-us/vstudio/>.

¹² Delphi developed by Embarcadero Technologies, <http://www.embarcadero.com/products/delphi>

The user can specify pipe properties, fluid properties, compressor properties, pressure set point thresholds, etc. It also gives the calculated pipe flows, compressor efficiency, compressor priorities, etc. as feedback.

Figure 43 shows a network setup for illustration purposes.

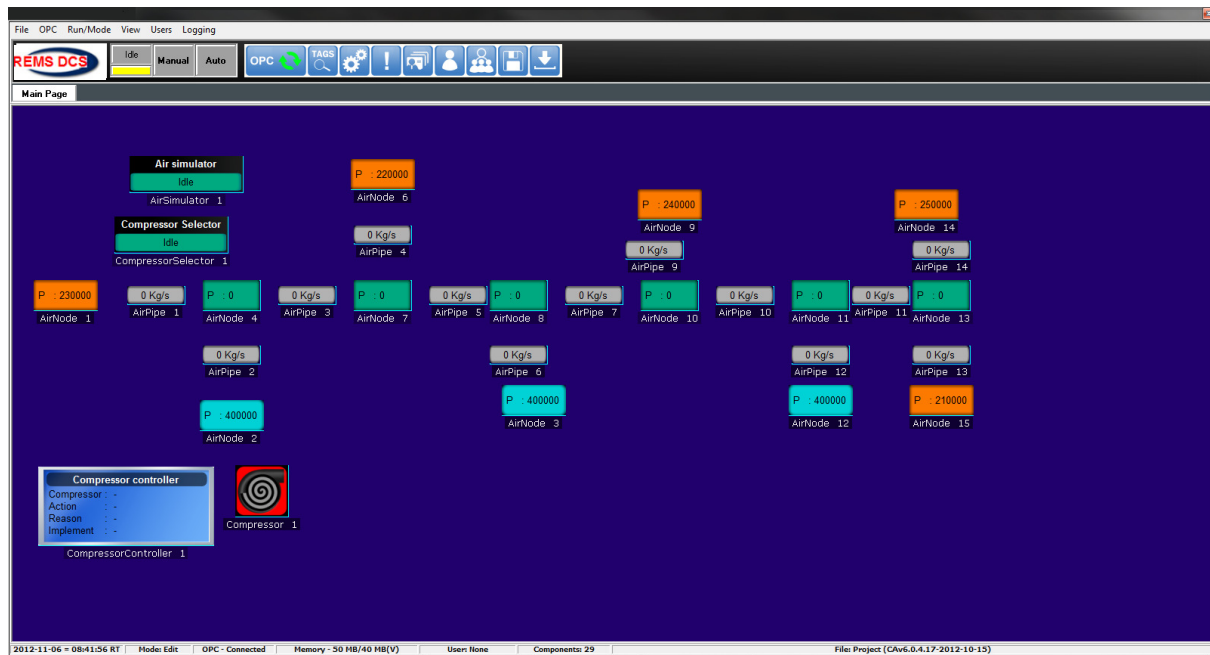


Figure 43: DCS overview

Each component's icon is drawn onto the main page window. These components include pipes, intermediate nodes, supply nodes, compressed air users and individual compressors. The user can arrange these icons as he or she sees fit.

Each component's properties can be modified by clicking on them and using their pop-up windows. The user is required to specify what each component is connected to. Figure 44 shows a tool that checks if all pipes and nodes are connected.

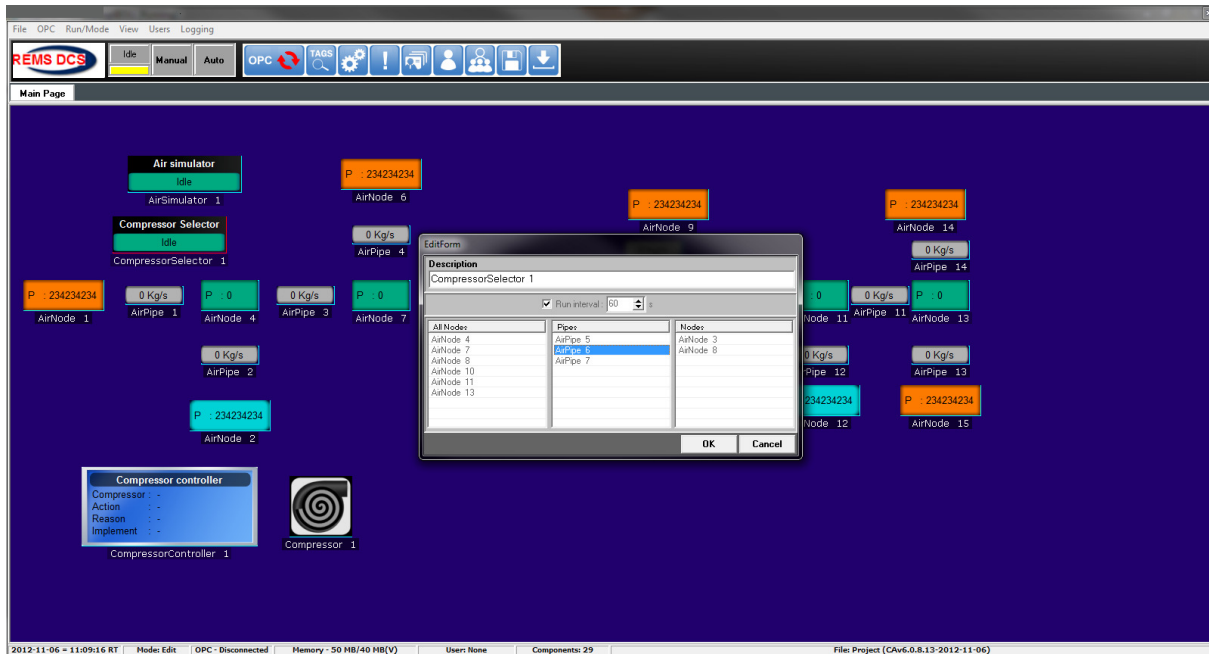


Figure 44: Compressor selector

To set up DCS, the user also specifies the types of nodes (intermediate, supply and demand) for the network, shown in Figure 45.

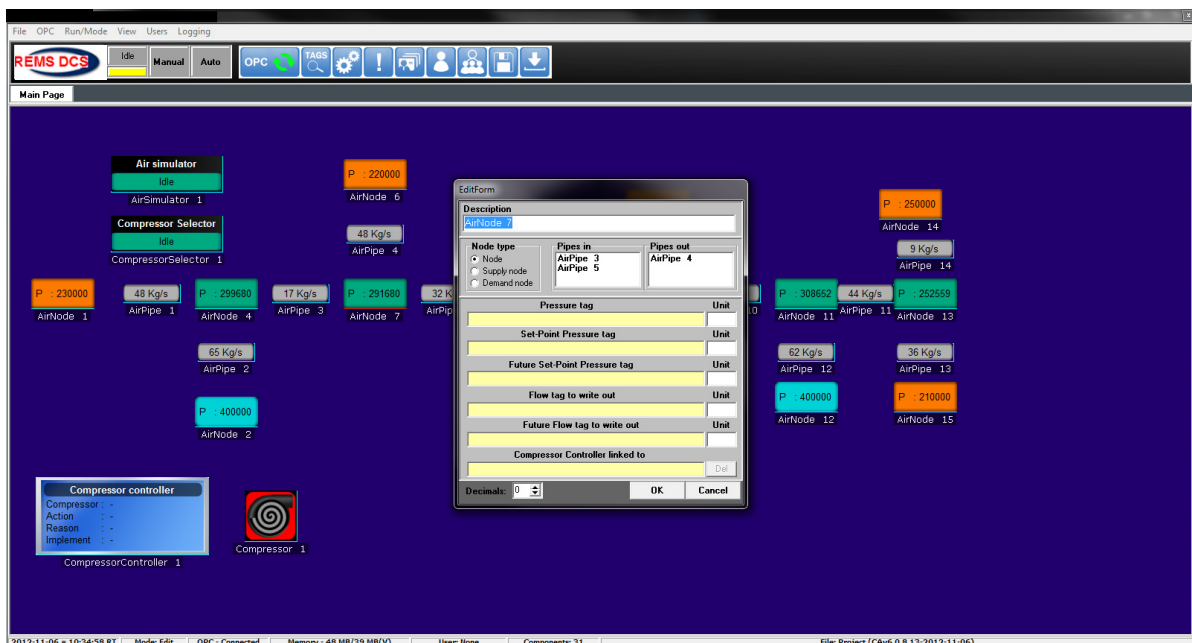


Figure 45: Node selection

The yellow spaces are where the user inserts network tags that enable the DCS to control and monitor.

Figure 46 shows the pop-up window for the pipe properties. Here the user can specify the pipe length, diameter, roughness and the geometry pipe pressure losses.

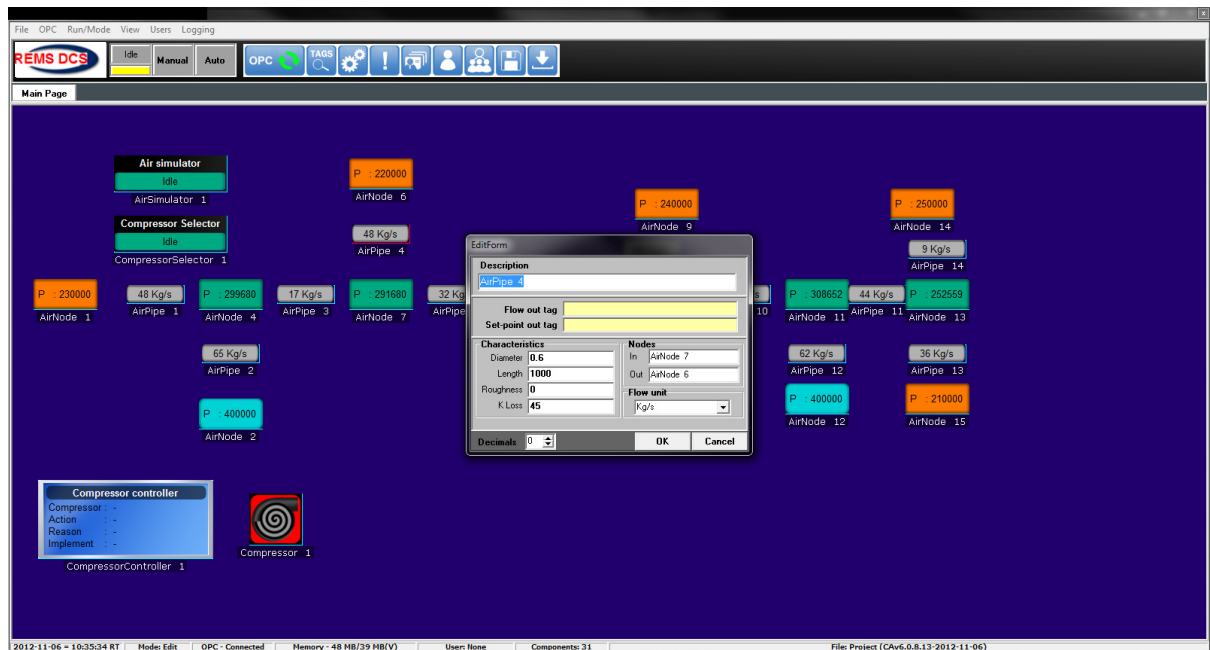


Figure 46: Pipe properties

Figure 47 shows the compressor properties for a single compressor. The user specifies at which compressor house this compressor located. The compressor characteristics are also given as input in this window. Tags that give compressor condition information are inserted into the yellow spaces.

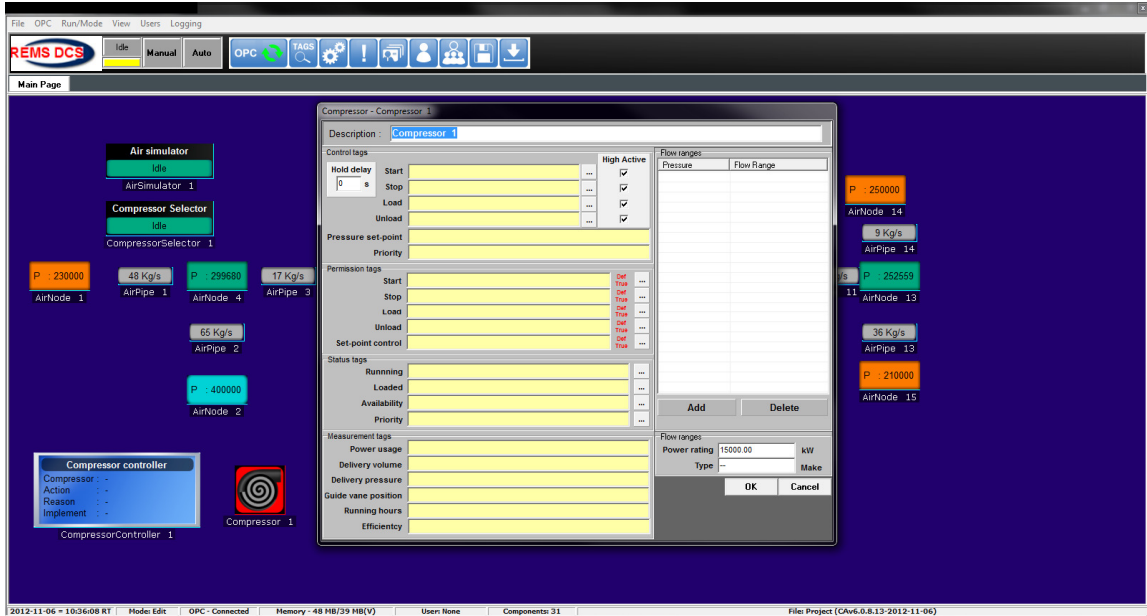


Figure 47: Compressor priorities window

Figure 49 shows the compressor controller that does the compressor prioritising and monitoring. This component receives results from the network-solving component. The network-solving component does not have a user interface.

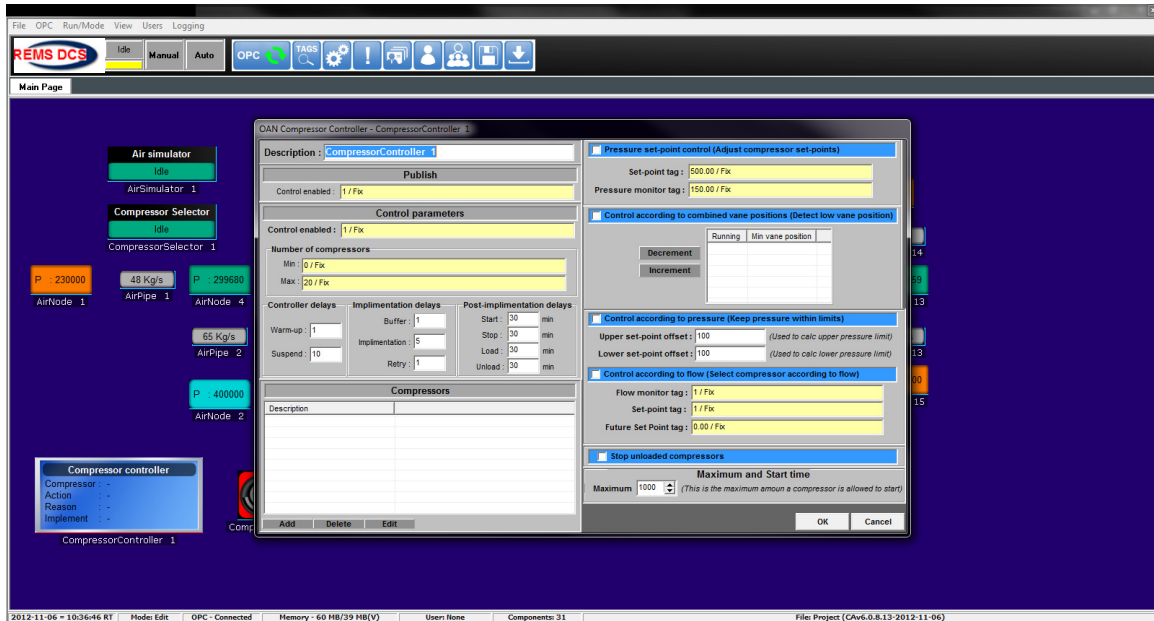


Figure 48: Compressor controller pop-up window

4.6 Conclusion

From the results in this chapter, it is possible to simulate compressed air networks accurately using the DCS.

It was also proven that the dynamic compressor selection method was an improvement on the present fixed priority compressor control method. Compressor cycling was reduced, but not eliminated.

The power consumption and flow demand for reduced shaft pressures were investigated. It was found that less power is consumed when shaft pressures and compressor set points are reduced outside of peak drilling times.

The proven abilities of the DCS contributed to it being integrated into the REMS platform.